Dynamics around the liquid-glass transition in poly(propylene-glycol) investigated by wide-frequency-range light-scattering techniques

R. Bergman
Department of Physics, Chalmers University of Technology, S-412 96 Göteborg, Sweden

L. Börjesson
Department of Applied Physics, Chalmers University of Technology, S-412 96 Göteborg, Sweden

L. M. Torell
Department of Physics, Chalmers University of Technology, S-412 96, Göteborg, Sweden

A. Fontana
INFM, Dipartimento di Fisica, Universita di Trento, 38050 Povo (Trento), Italy

(Received 25 October 1996)

The structural dynamics of poly(propylene-glycol) of molecular weight $M_W = 4000$ have been investigated over a large temperature range 10–375 K and in a wide dynamical window, corresponding to 10^{-3}–10^{14} Hz, using various light-scattering techniques. The slow dynamics were investigated using a wide time-range photon-correlation spectroscopy; for the faster dynamics a combination of interferometric and grating spectrometer techniques were used. We observe four distinguishable kinds of dynamics; (i) slow normal-mode dynamics, (ii) the main (α) relaxation which is related to the viscosity, (iii) a faster (β) relaxation, and (iv) a low-frequency vibrational peak. The data are discussed in relation to the mode-coupling theory (MCT) for the liquid-glass transition. Surprisingly, the slow dynamics observed using the PCS technique close to the glass transition temperature T_g are found to be in good agreement with predictions of MCT and a $T_c = 236$ K can be extracted. In contrast, the high-frequency data taken above T_c are not consistent with MCT. In this range a strong vibrational peak, the so-called boson peak, seriously affects the relaxational spectrum and simple MCT analysis cannot be applied. This finding is in agreement with recent light- and neutron-scattering investigations of other hydrogen-bonded intermediate glass formers and also strong covalently bonded systems. [S0163-1829(97)02042-0]

I. INTRODUCTION

The structural relaxation behavior of glass-forming liquids is currently a field of intense research, partly because of the success of recent theories to describe some characteristic features of the glass transition dynamics.[1] Experimentally the behavior above the glass transition temperature is dominated by the so-called α-relaxation (or main) process. The average relaxation time of the α process is closely related to the viscosity. It increases rapidly as the transition temperature is approached and generally in a non-Arrhenius fashion. The relaxation decays in a nonexponential manner normally well described by the Kohlrauch-Williams-Watts (KWW) stretched exponential,

$$\phi(t) = f \exp[-(t/\tau)^{\beta_{\mathrm{KWW}}}], \tag{1}$$

where τ is the relaxation time and β_{KWW} ($\leqslant 1$) is the so-called stretching parameter. The lower the β_{KWW} value the more stretched is the relaxation function. In the case of a KWW decay the average relaxation time is obtained through

$$\langle \tau \rangle = \frac{\tau}{\beta_{\mathrm{KWW}}} \Gamma(1/\beta_{\mathrm{KWW}}), \tag{2}$$

where Γ denotes the γ function. The temperature dependence of $\langle \tau \rangle$ is commonly described by the Vogel-Fulcher-Tammann (VFT) equation,

$$\langle \tau \rangle = \tau_0 \exp\left(\frac{DT_0}{T - T_0}\right), \tag{3}$$

where τ_0 is the fast relaxation time limit ($\approx 10^{-13}$–10^{-14} s) approached at ''infinitely'' high temperatures and D is a constant. According to Angell's strong-fragile classification scheme of glass-forming liquids the value of D determines the fragility of the system.[2] The lower the D value the less resistant (more fragile) is the system towards temperature-induced changes and the larger is the departure from Arrhenius behavior. T_0 is a fitting parameter indicating the temperature where the relaxation time (or viscosity) is expected to diverge. Interestingly, fits of experimental data of $\langle \tau \rangle$ or viscosity to Eq. (3) results in values of T_0 generally close to the so-called ideal glass transition temperature or the Kauzmann temperature, T_K. T_K is the temperature at which the supercooled liquid would reach an entropy equal to that of the corresponding crystal if the intervention of the glass transition did not occur. This is an unphysical situation known as the Kauzmann paradox. The experimentally determined calorimetric glass transition temperature, T_g, is commonly defined as the temperature at

which the relaxation time has reached a value of ≈ 200 s, i.e., $\tau(T_g) \approx 200$ s. It follows from Eq. (3) that $T_g > T_0$ and that the difference between the experimental and ideal value increases as the ''strength'' of the liquid increases:

$$T_g = T_0\left(1 + \frac{D}{\ln[\tau(T_g)/\tau_0]}\right) \approx T_0\left(1 + \frac{D}{36.4}\right), \qquad (4)$$

D being typically ≈ 5 for liquids of the fragile extremes and $D > 30$ for strong systems.[3]

A theoretical explanation of the glass transition dynamics which has received much attention during recent years is given by the mode coupling theory (MCT).[4] Based on a microscopic approach MCT relates the glass transition to yet another temperature, T_c, defined by the arrest of diffusional motion of the individual atoms or molecules of the system as the temperature decreases. Lowering the temperature further, $T < T_c$, the molecules will be trapped in cages formed by their neighbors. According to the first simplified MCT version[5–7] the viscosity (η) and the accompanying main ($\alpha-$) relaxation time, show critical divergence at T_c described by a power law

$$\eta \propto \tau_\alpha \propto (T - T_c)^{-\gamma}. \qquad (5)$$

MCT makes further explicit predictions of the shape of the relaxation function as discussed in the next paragraph. Many of the theoretical predictions have been proven valid in experimental tests of real glassformers[8] although MCT was originally developed for the mathematically idealized case of a hard-sphere system. In the experimental verifications of MCT it turns out that the critical temperature T_c is to be found much above the calorimetrically determined transition temperature, T_g, and thus the theory has shifted a substantial part of the interest for experimental observations of glass transition phenomena to higher temperatures and also to shorter times ($<$ns). Intense experimental activities have followed the theoretical development of the MCT theory.[1] It is demonstrated that MCT is particularly successful in describing the dynamics of glass formers resembling hard-sphere systems such as colloidal suspensions[9,10] and also ionic and molecular systems which represent fragile extremes of Angell's classification scheme.[11–13] For intermediate and strong glass formers experimental results for the structural relaxation dynamics appear to qualitatively follow the MCT predictions.[14–16] However, it seems that for the stronger glass formers the theory fails to describe the dynamics at high frequencies and it has been explained by the strong vibrational contributions present in these systems. Moreover, it seems in retrospect that vibrational states contributes to the relaxation scenario also in the case of the fragile glass formers, though the deviations from MCT behavior is much smaller.[15] MCT has been theoretically further developed for such complicated systems as polymers.[17,18] Again the main features of the original theory prevail and have for a few cases been experimentally confirmed.[19,20]

A general problem in testing the MCT theory is the wide dynamical range needed to be able to experimentally follow the relaxation dynamics of a glass former. In this work we combine dynamic light scattering techniques which enable us to follow the dynamics over a time range of 16 decades. The study concerns a polymeric glass former, poly(propylene glycol) (PPG), of low molecular weight ($M_W = 4000$) corresponding to approximately 68 repeat units. The relaxation behavior of PPG has been probed using photon correlation spectroscopy (PCS) together with combined depolarized Raman and Brillouin spectroscopy by which the enormous dynamical range 10^{-12}–10^4 s is covered. Using such a wide time range we aim particularly to follow the influence of the vibrational contributions on the relaxational processes as the system is cooled from the liquid state over the supercooled regime to the glass. Some of the PCS results of PPC have been reported previously[21] while the Raman and Brillouin data are new.

II. MODE COUPLING THEORY PREDICTIONS

Above the critical temperature, T_c, mode coupling theory[1] suggests a two-step decay of the relaxation function of density fluctuations, $\phi(t)$, generally being referred to as the β and the α processes, respectively. The faster of the two, the β process, is expected to decay between microscopic times and a certain crossover time, t_1, towards an intermediate relaxation level of the system defined by the so-called nonergodicity parameter f_q^c. The last part of this decay is in MCT expressed by a power law, $\phi(t) - f_q^c = h_q(t/t_0)^{-a}$, where t_0 is a temperature-independent time constant and h_q is the so-called critical amplitude. h_q as well as f_q^c are predicted to be smooth and positive functions of the wave vector q. The second step of the decay is dominated by the α process, which occurs at longer times and by which $\phi(t)$ decays from f_q^c to 0. The initial part of the second step is predicted to follow a von Schweidler decay, $\phi(t) - f_q^c \propto -(t/\tau)^b$, while at longer times it is well described by the KWW function [Eq. (1)]. It is the relaxation time of this process that is predicted to diverge at T_c [see Eq. (5)]. Around the f_q^c level $\phi(t)$ is approximately described by an interpolation formula:

$$\phi_{\rm int}(t) = f_q^c + A_\sigma[(t_1/t)^a - (t/t_1)^b], \qquad (6)$$

with the exponents being within the range $0 < a < 0.4$ and $0 < b \leq 1$. For a more accurate analysis of the behavior around the nonergodicity level f_q, higher-order terms should be included in Eq. (6). In the present work we will however use Eq. (6) based on only the leading terms for discussing the experimental data.

The relaxation function can experimentally be probed using time domain techniques, such as for instance photon correlation[22] or spin-echo neutron-scattering[19] methods, by which one can directly measure $\phi(t)$. Alternatively, the dynamics can be probed in the frequency domain using other techniques such as quasielastic neutron scattering or depolarized light (Raman and Brillouin) scattering. Then the relaxation dynamics is conveniently expressed by the dynamical susceptibility, $\chi''(\omega)$. Transforming Eq. (6) to the frequency domain, $\chi''(\omega)$ will exhibit a minimum between the two power-law asymptotic regions, defined by exponents a and $-b$ at high, respectively, low frequencies. The MCT scenario around the minimum in the susceptibility spectrum, for $T > T_c$, is schematically shown in Fig. 1 and the corresponding interpolation formula is given by

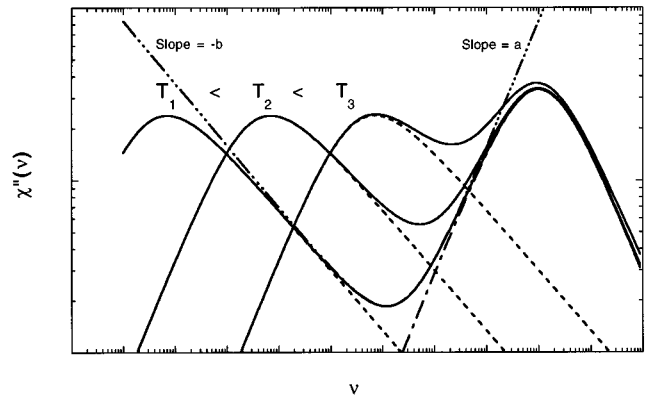

FIG. 1. Schematic picture showing the combined effects on the susceptibility of two relaxation processes as one of the processes (the lower-frequency one) moves towards higher frequencies with increasing temperature. The higher-frequency process is temperature independent. Dash-dotted curve represents the interpolation formula of Eq. (7).

$$\chi''(\omega)=\frac{\chi''_{\min}}{a+b}\left[b\left(\frac{\omega}{\omega_{\min}}\right)^{a}+a\left(\frac{\omega}{\omega_{\min}}\right)^{-b}\right], \tag{7}$$

where the parameters a and b are the same as in Eq. (6). The parameters $\omega_{\min}$ and $\chi''_{\min}$ define the minimum which changes as the temperature changes and the α relaxation (the low-frequency peak in Fig. 1) slides along the frequency axis. The behavior of the high-frequency side of the minimum is supposed to be only weakly temperature dependent which results in the following relations:

$$\omega_{\min}\propto\omega_{\alpha}^{b/(a+b)} \tag{8}$$

and

$$\chi''_{\min}\propto\omega_{\alpha}^{ab/(a+b)}, \tag{9}$$

where $\omega_{\alpha}\propto 1/\tau_{\alpha}$ defines the peak position of the α relaxation. From Eqs. (8) and (9) we obtain a relation that can be used to determine the a exponent

$$\chi''_{\min}\propto\omega_{\min}^{a}, \tag{10}$$

without any assumption of the temperature dependence of ω_{α}. The temperature dependence predicted by MCT is given by the power-law behavior of Eq. (5), with the exponent γ related to the exponents a and b according to

$$\gamma=\frac{1}{2a}+\frac{1}{2b}. \tag{11}$$

Using Eqs. (8), (9), (11), and (5) MCT suggests the following temperature dependencies for the parameters of the minimum:

$$\omega_{\min}\propto\frac{1}{t_1}\propto(T-T_c)^{1/2a}, \tag{12}$$

$$\chi''_{\min}\propto A_{\sigma}\propto(T-T_c)^{1/2}. \tag{13}$$

The exponents a and b are apart from Eq. (11) predicted to be closely related through the common value of the coupling parameter λ:

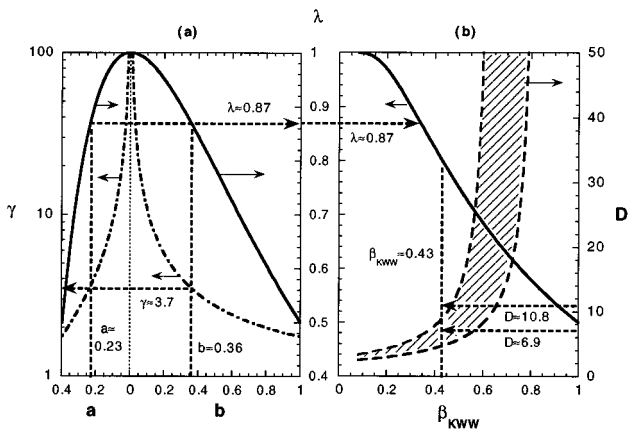

FIG. 2. Graphic representation of (a) the relation between the exponents a, b, γ, and λ of MCT [Eqs. (5), (11), and (14)] and, (b) the empirical experimentally found correlation between VFT and KWW functions, Eqs. (2) and (3) (shaded area), see text. The present results obtained for PPG using PCS are indicated (dashed lines and arrows).

$$\lambda=\frac{\Gamma^2(1-a)}{\Gamma(1-2a)}=\frac{\Gamma^2(1+b)}{\Gamma(1+2b)}. \tag{14}$$

Equations (11) and (14) relate the temperature evolution of the relaxation (determined by exponent γ) with the actual shape of the time decay (determined by exponents a and b) and are key equations in experimental tests of the MCT predictions. A graphical representation of the two equations relating γ and λ to a and b are presented in Fig. 2(a). It is obvious that one can obtain all the parameters a, b, γ, or λ by just measuring one of them. However, Fig. 2(a) shows that uncertainties in the experimental determination of the a-parameter result in much larger uncertainties for the other parameters than determining the b parameter for obtaining γ or λ. A more solid route for a test of the MCT is to measure both the a and b parameters independently and then test Eq. (14) for a common λ value and if so test whether the γ value obtained though Eq. (11) can describe the temperature evolution of the viscosity and α-relaxation time.

It is interesting to note that MCT predicts a close relation between the shape of the relaxation function [Eq. (6) or (7)] and the temperature dependence of the relaxation time or viscosity [Eq. (5)]. As γ gives the steepness of the curve in the relaxation time vs $1/T$ plot it can be viewed as a measure of the fragility just as the D parameter of the VFT equation [Eq. (3)]. Indeed, Böhmer *et al.*[3] have recently shown that for a wide range of systems there is experimental evidence for a correlation between the fragility m, expressed as the slope at T_g in a $\log_{10}\langle\tau\rangle$ vs T_g/T plot

$$m=\left.\frac{d\,\log_{10}\langle\tau\rangle}{d(T_g/T)}\right|_{T=T_g}\approx 16+\frac{590}{D}$$

and the nonexponentiality (expressed by β_{KWW}) of the relaxation function. In Fig. 2(b) we show the approximate relation obtained experimentally connecting β_{KWW} at T_g and the D parameter. The β_{KWW} value of the KWW function [Eq. (1)] describing the α relaxation is usually close to the b value of MCT and therefore related to λ. An approximate relation

connecting β_{KWW} to λ has been given by Kim and Mazenko,[23] $\beta_{KWW} = -\ln(2)/\ln(1-\lambda)$, and it is included in Fig. 2(b). Figure 2(b) then gives the opportunity to relate the MCT parameter λ to both β_{KWW} and D, the traditional parameters used to describe the non-Debye and non-Arrhenius behavior of glass formers. Then by combining Figs. 2(a) and 2(b) which have a common λ axis, it is possible to compare all MCT parameters with the traditional parameters β_{KWW} and D. We note, however, that experimental data of β_{KWW} often reveal a temperature dependence[24–26] such that comparisons using Fig. 2 should be performed with caution.

The viscosity is in the original simplified MCT representation suggested to diverge at the critical temperature, T_c. There are however no experimental evidence of any critical behavior of the viscosity but rather there seems to be a smooth crossover from a high-temperature region where Eq. (5) holds to a low-temperature region $T < T_c$ where the temperature dependence is close to Arrhenius. A smooth crossover can theoretically be obtained by incorporating activated hopping processes as possible motions below T_c when the molecules are caged by their surroundings. In the so extended MCT (Ref. 4) the hopping processes are accounted for by an extra parameter δ in the memory function. It implies that also below T_c a two-step decay of the relaxation function and a minimum of the susceptibility is expected.

On the other hand, Yeo and Mazenko[27] have shown that by introducing defect fluctuations which couple to density fluctuations, the MCT scenario is altered such that there is no evidence of any critical temperature, T_c. Moreover, such a coupling leads to a temperature-dependent λ value and therefore to temperature-dependent a, b, and γ values. This in turn implies a temperature dependence of the stretching parameter, β_{KWW}, which has been observed to be the case for many experimental systems.[24–26] We also note that Schmitz *et al.*[28] have derived another version of MCT in which again the sharp transition of the original MCT is absent.

III. EXPERIMENT

PPG (MW 4000) purchased from Polyscience Inc. was dried at 70 °C in a vacuum oven for several days and then degassed by repeated freeze-dry cycles on a vacuum line. This procedure effectively eliminates water and any low MW PPG residual from the polymerization. The rather viscous PPG was then forced through a 0.22-μm filter (Millipore) directly into a clean square optical cuvette used for the light-scattering experiments.

Photon correlation experiments were performed on the PPG sample to probe the relatively slow relaxational dynamics around the calorimetric glass transition. During the measurements the sample was kept in a liquid-nitrogen cold-finger cryostat (Oxford Instruments). The accuracy of the temperature measurement is estimated to be ± 0.5 K. An Ar^+ laser (Spectra Physics), operating at 488 nm with an output power of ~ 500 mW, provided the incident radiation. Light scattered at an angle of 90° was detected, digitized, and fed to a correlator (ALV-5000) which covers the wide range of about 12 decades in time. The correlator calculates the normalized autocorrelation function of the scattered intensity which, in case of homodyne detection, is related to the field correlation function, $g_1(t)$, by

$$\frac{\langle I(t)(I(0)\rangle}{\langle I\rangle^2} = 1 + \sigma |g_1(t)|^2, \tag{15}$$

where σ is the instrumental coherence factor (≈ 0.9). In the present study of relaxation dynamics of a polymeric glass-former $g_1(t)$ can be identified as the relaxation function $\phi(t)$ addressed by MCT since the scattered field is mainly caused by density fluctuations in the sample.[29]

For investigations of the faster dynamics frequency domain measurements were performed using a four-pass grating spectrometer (Sopra DMDP 2000) and a tandem Fabry-Perot interferometer (Sandercock). The measurements were made in a helium cryostat for low temperatures and in an oven for the high temperatures. The temperature stability was better than ± 1 K in each case. Depolarized light-scattering measurements were done using either the 488 nm or the 514 nm line of an argon laser with a power less than 500 mW. The grating spectrometer measurements were taken in the temperature range 10–375 K using three different slit widths in order to cover the frequency range 10–6000 GHz without any influence of elastically scattered light. The interferometric measurements were performed only above room temperature using three different free spectral ranges (10, 30, and 90 GHz, respectively) of the interferometer, which had a finesse of about 100. The different grating spectrometer and interferometer spectra were matched to each other using the overlapping frequency regions. The obtained frequency spectrum $I_{expt}(\nu)$ is related to the imaginary part of the light-scattering susceptibility $\chi''(\nu)$ through

$$\chi''(\nu) \propto I_{expt}(\nu)/[n(\nu,T)+1], \tag{16}$$

where $n(\nu,T)$ is the Bose-Einstein population factor.

IV. RESULTS

A. Time domain results (PCS)

In Fig. 3 we present the previous PCS results of the density correlation functions $\phi(t)$ for PPG reported from this laboratory[21] together with present measurements. Spectra were obtained over the temperature range 186–221 K. The relaxation function is for almost the whole time range and for all temperatures studied well described by the KWW stretched exponential, Eq. (1), with $\beta_{KWW} \approx 0.39$ and with a relaxation time that rapidly increases as temperature decreases, see Fig. 4. For comparison we include in Fig. 4 data for the average relaxation time reported for the α process from dielectric measurements[30,31] and from Brillouin[32] and impulsive stimulated light scattering (ISS) spectroscopy.[33] As can be seen in Fig. 4 the data for $\langle\tau\rangle$, as also for β_{KWW}, are in accordance with those of the main relaxation process in PPG and we conclude that the dominant relaxational feature observed in the PCS study is the α process. However, at short times there are deviations from the KWW fits (see inset of Fig. 3) which indicates the presence of some faster relaxation process, e.g., the so-called β relaxation of MCT. Although these observations are made at the short-time limit of the PCS window and the experimental scatter is large the deviations are significant and systematic. The origin of this short time deviation is probably due to a relaxation with a shorter relaxation time than the PCS time window allows us

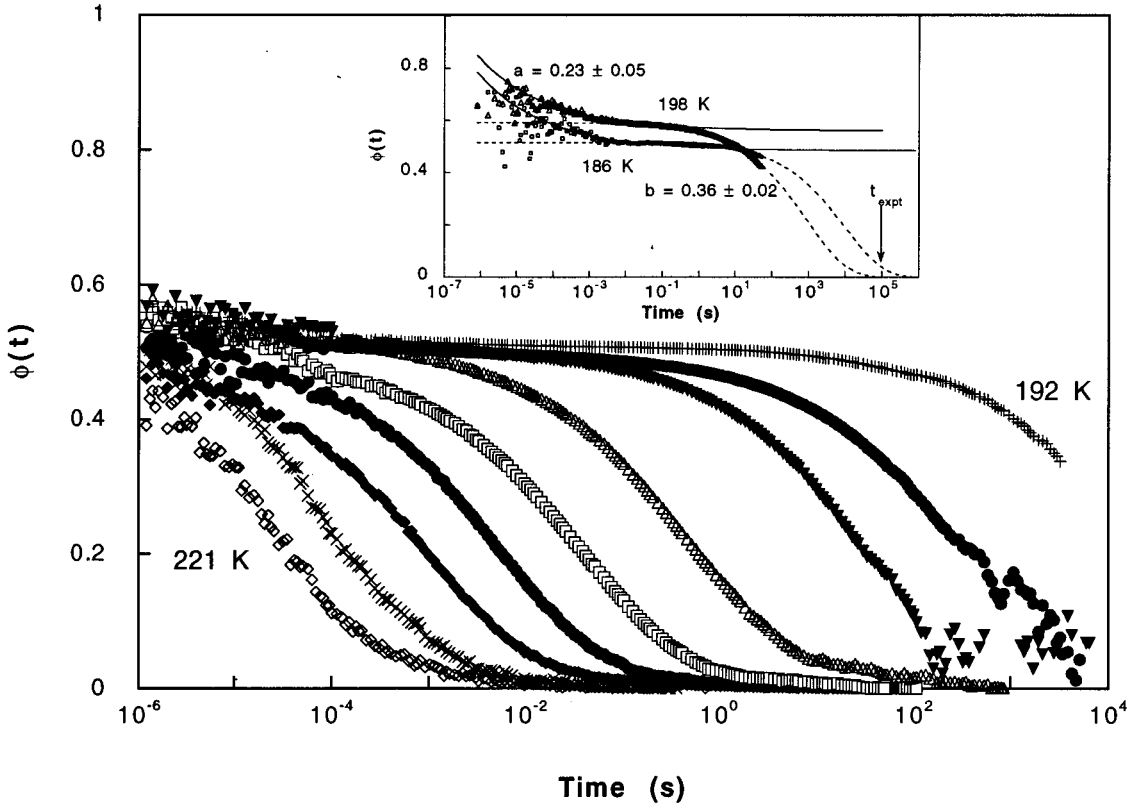

FIG. 3. Relaxation functions obtained for PPG (4000) by PCS in the temperature range 192–221 K (192, 198, 200, 205, 208, 211, 214, 218, 221 K). Inset shows data taken below T_g which display a second short-time relaxation step. Dashed lines represent KWW [Eq. (1)] extrapolations to longer times. Full lines represent power-law decays towards the nonergodic level. The total experimental time is indicated by the arrow.

to determine. However, its long-time tail can still be seen in our time window. Using a two-step relaxation approach, according to the MCT, the short-time behavior can be described by a power-law decay towards the nonergodicity level and thereafter another power-law decay follows describing the slower α process. The obtained exponents $a = 0.23 \pm 0.05$ and $b = 0.36 \pm 0.02$ of such an analysis (see inset of Fig. 3) fulfills the MCT relation Eq. (14) and gives $\lambda \approx 0.87 \pm 0.02$ and $\gamma \approx 3.6 \pm 0.2$ as shown in Fig. 2(a). The resulting uncertainties of λ and γ are based on the rather well-defined b value, whereas the errors of the a value will give significantly larger uncertainty. The so obtained λ and γ results are consistent with a MCT analysis[20] of dielectric data of PPG (Ref. 34) and describe the high-temperature behavior of the viscosity with $T_c = 236 \pm 2$ K (see inset of Fig. 3 of Ref. 21).

A Vogel-Fulcher-Tammann (VFT) equation, Eq. (3), was fitted to the present data for the relaxation times of the α process and previously reported Brillouin and ISS data.[33] We obtain $T_0 = 157$ K and $D = 10.8$, see full line in Fig. 4, the latter indicating that PPG is a glass former of intermediate fragility. The fit gives however a somewhat low value for the preexponent, $\tau_0 = 10^{-15.2}$ s. High-quality dielectric data for the α-relaxation times are best fit using $D = 6.7$ and $T_0 = 165$ K.[31] Thus, the dielectric data differ significantly from the present light scattering data, in particular in the high-temperature range. Similar findings have been observed in other glass formers.[25]

MCT suggests that the high-temperature α-relaxation time follows a power law, Eq. (5), and it is represented in Fig. 4 as a dotted line. The latter was generated using $T_c = 236$ K as obtained from the fit to viscosity data with $\gamma = 3.6$ determined from the measured exponents a and b, Eq. (6). It can be seen that the power law provides excellent fit to the high-temperature ($T > T_c$), light-scattering data. As the α process does not freeze at T_c, the VFT function provides a better fit over the whole relevant time-temperature range.

At higher temperatures we notice another deviation from the KWW behavior present as a tail at the long-time end of the α process. The deviation is more clear in the representation of Fig. 5 where we show the $\phi(t)$ data subtracted by a KWW function, the function used was obtained from fits of $\phi(t)$ omitting the tail at the long-time end. While the original complete $\phi(t)$ curves are best fit using a β_{KWW} value of ≈ 0.39 the ones used for subtractions, i.e., excluding the long-time tail, are better characterized by $\beta_{\mathrm{KWW}} \approx 0.43$ [indicated with a dashed line in Fig. 2(b)]. The results in Fig. 5 show a residual decay of $\phi(t)$ with a characteristic relaxation time exceeding that of the α process with more than one decade. Furthermore, the residual decay seems to be less distributed ($\beta_{\mathrm{KWW}} \approx 0.7$) than the α relaxation though the huge experimental scatter of the data only allow rough estimations. This uncertainty naturally imply enormous error bars on $\langle \tau \rangle$.

In Fig. 4 we include the average relaxation times estimated for the residual decay which exhibits roughly the same

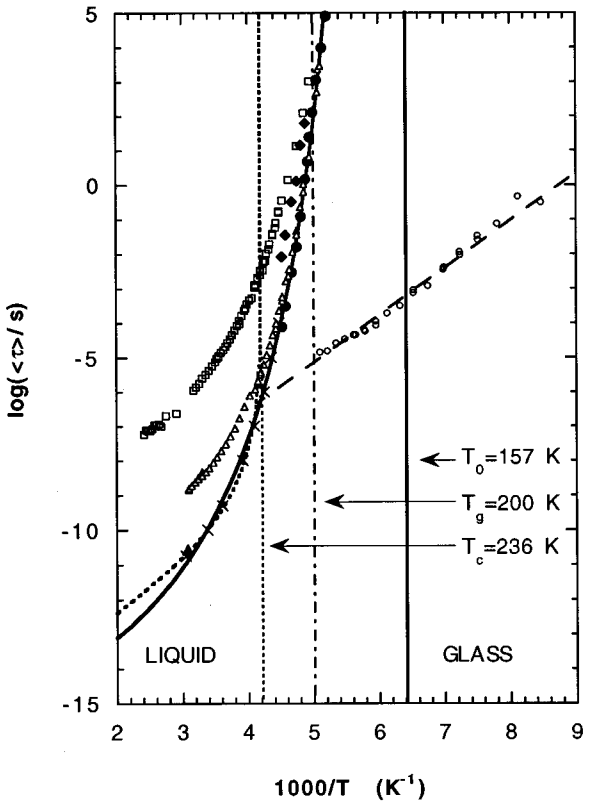

FIG. 4. Arrhenius plot of the mean relaxation times for PPG (4000). Photon correlation data for the main α process are marked with filled circles, whereas data for the α' relaxation are marked with filled diamonds. ISS (Ref. 33) and Brillouin data (Ref. 32) are marked with crosses and a filled triangle, respectively. Dielectric data reported by Schönhals *et al.* (Refs. 30 and 31) for the α', α, and β relaxations are marked with open squares, open triangles and open circles, respectively. Solid curve represents a fit of the VFT equation [Eq. (3)] to the α process observed with the different light-scattering techniques, the dotted curve represents a fit of the MCT power law [Eq. (5)] to the high-temperature data and the dashed curve represents an Arrhenius equation through the dielectric β relaxation data.

temperature dependence as the normal mode or α'-relaxation process measured by dielectric spectroscopy, the latter being attributed to the motions of whole chains through the fluctuations in the end-to-end vector.[30] We thus attribute the slow residual decay to motions of the whole chains.

B. Frequency domain results

Spectra in the high-frequency range $\nu > 1$ GHz, obtained by combining depolarized Brillouin and Raman spectra are shown in Fig. 6. The spectra in Fig. 6 are shown in a scaled representation $I(\nu) = I_{\text{expt}}(\nu)/\{\nu[n(\nu,T)+1]\}$, where $n(\nu,T)$ is the Bose-Einstein population factor, to reduce for trivial temperature induced population effects. It can be seen in the figure that at low temperatures the spectrum is completely dominated by a broad assymetric vibrational mode, the so-called boson peak which has been observed for most disordered amorphous materials. With increasing temperature a quasielastic contribution grows continuously and it dominates completely the spectrum for the higher temperatures. In Fig. 7(a) we show the data in the susceptibility form and in Fig. 7(b) the data are scaled such that the minima overlap. The scaling is performed by dividing the frequency and the susceptibility data with the corresponding values at the

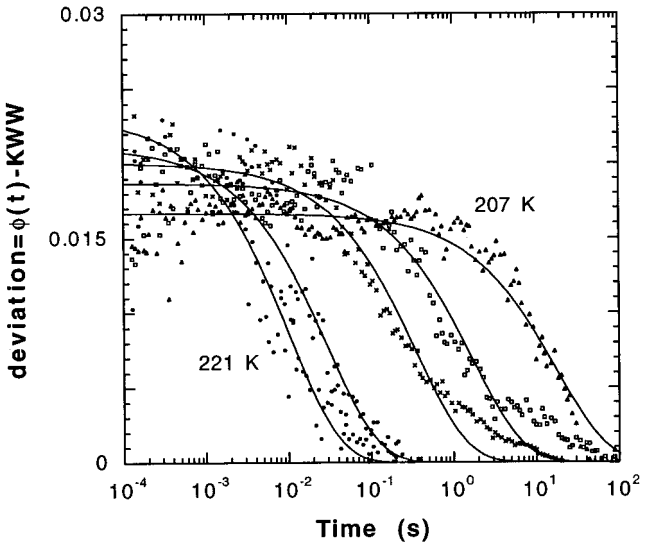

FIG. 5. Deviation of the long-time part of the relaxation function from a KWW behavior [Eq. (1)] showing the existence of an additional long-time process. Solid curves represent fits to the data with a KWW function using $\beta = 0.7$.

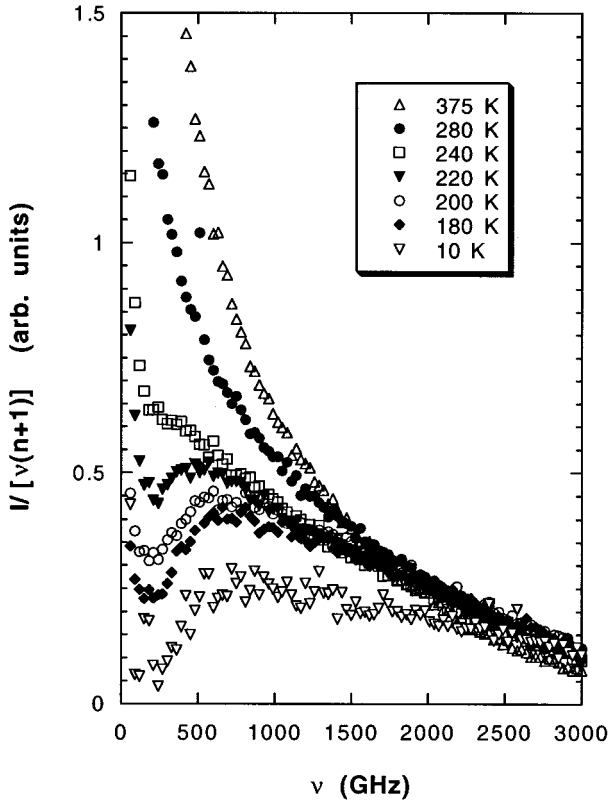

FIG. 6. Depolarized Raman scattering data of PPG (4000) in the temperature range 10–375 K. Experimental intensities have been corrected for the Bose-Einstein population factor.

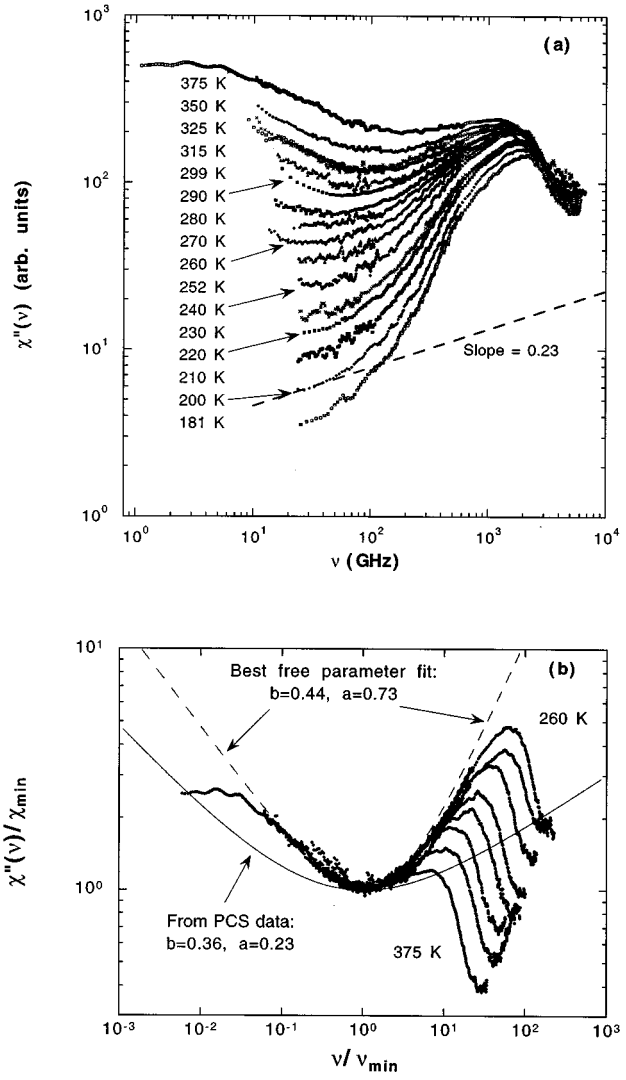

FIG. 7. (a) Susceptibility spectra $\chi''(\nu)$ for PPG (4000) from depolarized light scattering using a combination of interferometric and grating techniques. (b) Master plot of the data in (a) scaled such that the minima coincide. The solid curve represents the MCT interpolation formula, Eqs. (7) and (14), using λ as determined by PCS. The dashed curve represent a free fit to Eq. (7), i.e., a and b are not restricted by Eq. (14).

minima, such that the region around the minima could be described by a master function. According to the MCT predictions the spectra in Fig. 7 should adhere to the interpolation formula, Eq. (7), with exponents a and b related through Eq. (14). The best free fit (dashed line) to the minima of the master function gives $a \approx 0.73$ and $b \approx 0.44$. It is obvious that the a and b values, obtained above from lower frequencies using the PCS technique fail to describe the susceptibility master curve, see the full line in Fig. 7(b). In fact the a value obtained from the fit to the master curve (≈ 0.73) is higher than the limiting value (≈ 0.395) in the MCT. Another approach to obtain the exponent a is to plot $\log_{10} \chi''_{\min}$ versus $\log_{10} \nu_{\min}$, and according to Eq. (10) a is then given by the slope. Such a plot is shown in Fig. 8 and from the slope we obtain $a \approx 0.75$, i.e., close to the value obtained from the fit to the master curve in Fig. 7(b) as expected. We note, however, that the construction of a master curve can hide temperature dependencies of the exponents a and b, which would be in conflict with MCT. Indeed, fitting each spectrum individually reveals a temperature dependence of the a exponent, see inset of Fig. 8, contrary to the MCT predictions. Moreover we find that also the b exponent exhibits a temperature dependence. Interestingly, we note that the value of b obtained by the combined depolarized Brillouin-Raman technique approaches that obtained by the PCS technique ($b \approx 0.36$) at lower temperatures where a larger part of the α relaxation is seen in the time window. Thus we note that the α relaxation can indeed be described by approximately the same exponent over the whole relevant time-frequency range while this is not the case for the fast dynamics of the β process.

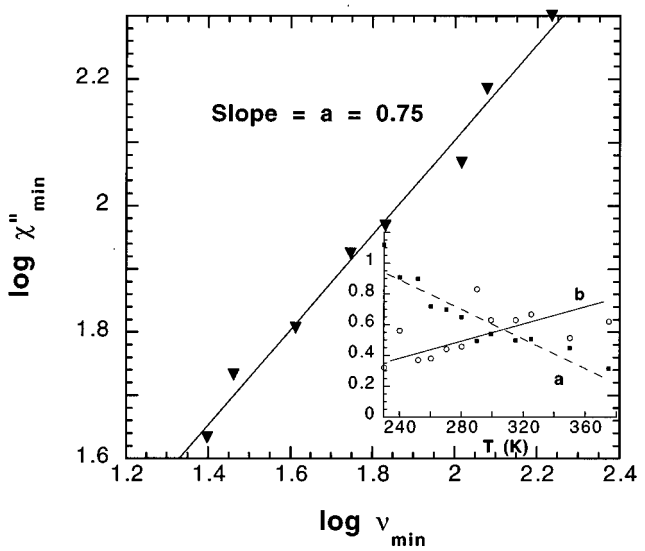

FIG. 8. Double-logarithmic plot of $\chi''_{\min}$ vs $\nu_{\min}$. The solid line represents a linear fit with slope $a_{\text{eff}} = 0.75$. The inset shows the temperature dependence of the a and b parameters as obtained from free fits.

According to Eqs. (12) and (13) $\nu_{\min}^{2a}$ and $\chi''^{2}_{\min}$ should have a linear temperature dependence and extrpolate to zero at T_c. Using $a = 0.73$ as obtained from the fit to the master curve we obtain $T_c \approx 265$ K which is ≈ 30 K above the reported T_c. If we instead use $a = 0.23$, as obtained in our PCS study, we obtain, from Eq. (12), $T_c \approx 180$ K which is clearly below T_g. It is obvious that the contribution from the boson peak has to properly be taken into account before a quantitative MCT analysis can be performed on the susceptibility data of PPG.

V. DISCUSSION

A. The α and β relaxations

Above T_c we obtain, by fitting the susceptibility to the suggested interpolation formula Eq. (6), temperature dependent a and b values, though it is possible to construct a master curve with $a = 0.73$ and $b = 0.44$ see Fig. 7(b). These values do not give the same λ, see Fig. 2(a), and the a value is higher than allowed within the MCT. The position of the minima follow Eq. (10) with a practically identical a value, however, it does not follow Eqs. (12) and (13). The failure to obey the MCT scaling relations seems to be related to sig-

nificant influence of vibrational dynamics, i.e., the presence of a strong boson peak. Similar findings have been reported for other nonfragile network forming glassformers in which the vibrational dynamics is much more pronounced than in fragile non-network systems.

As the minimum in $\chi''(\nu)$ moves to lower frequencies and out of the influence of the boson peak when temperature is decreased one would expect that the MCT picture holds. Unfortunately, we can not follow the minimum below 260 K in the frequency representation due to the limited dynamical range of the spectrometer. However, using PCS, it is possible to measure $\phi(t)$ at long times corresponding to considerably lower frequencies. As seen above we observe the α relaxation at $T<T_c$, i.e., it is not arrested at T_c as suggested in the ideal MCT. According to MCT such a deviation may be caused by hopping processes or coupling between density and defect fluctuations which smooth the transition.[4,35] Then MCT predicts that below T_c the short-time dynamics are still ruled by a critical decay with the exponent a unchanged[4,35] and, thus, the two-step scenario suggested above T_c should be valid also below T_c. Although the β process is assumed to contribute mainly to short times, i.e., close to a microscopic vibrational time, its long-time tail may be visible in the PCS time window. Such a picture can explain why we can see the predicted two-step behavior at $T<T_c$ in PCS with exponents a and b fulfilling the MCT relationship and also describing the viscosity behavior at $T>T_c$ [Eqs. (5), (11), and (14)]. It furthermore suggests that for glass forming systems exhibiting a strong boson peak, generally nonfragile ones, the MCT two-step relaxation decay scenario may paradoxically be best studied below T_c since then the relaxation processes are slow and the minimum of $\chi''(\nu)$ is far away from the Boson peak. Indeed, as indicated by the dashed line in Fig. 7(a) it seems as if the low-frequency end of the low-temperature $\chi''(\nu)$ data (close to $T_g=200$ K) can be described by a power law with the exponent close to the one obtained in the analysis of the PCS data ($a\approx 0.23$).

Deviations from the predicted MCT behavior of the high-frequency β relaxations have been reported for several intermediate and strong glasses[14–16] and also, but less pronounced, for fragile systems.[15] In Fig. 9 we plot the values for the ratio $a_{\rm eff}/a_{\rm MCT}$ vs the fragility (m), where $a_{\rm eff}$ is the value obtained from the fit of the minum parameters and $a_{\rm MCT}$ is the value corresponding to the b-value according to the MCT relation Eq. (14). As seen in the figure the ratio increases slowly for decreasing fragility for the nonhydrogen bonded systems $Ca_{0.4}K_{0.6}(NO_3)_{1.4}$, orthoterphenyl, m-tricresyl-phosphate, salol and B_2O_3, while for the hydrogen bonded materials glycerol and PPG (4000), the deviations are even larger than this general trend.

In Fig. 10 we show the present susceptibility data together with the PCS data transformed to $\chi''(\nu)$ in order to give the full picture of our data in one figure. The PCS data of the α relaxation is plotted as Havriliak-Negami functions obtained using the fitted KWW parameters and the relation between Havriliak-Negami and KWW parameters found by Alvarez *et al.*[36,37] The figure is constructed to give a pictorial view of the dynamics involved in the glass transition in PPG (4000). Compared with the MCT scenario in Fig. 1 there are many similarities but also differences. The most important deviation is that the intensity in the fast relaxation range decreases strongly with decreasing temperature also below T_c. Note that the decrease is not related to the ''knee'' as predicted by MCT to occur below T_c as crossover between the fast relaxation and the white noise spectrum. Thus, at $T<T_c$ there is a marked deviation from the MCT scenario even on a qualitative level.

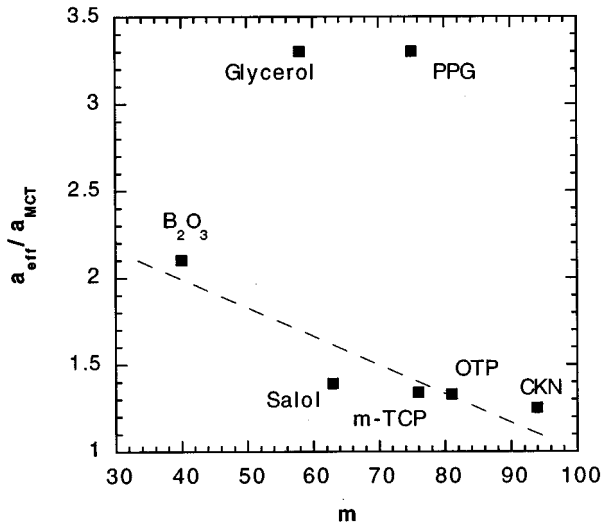

FIG. 9. Values of $a_{\rm eff}/a_{\rm MCT}$ vs the fragility m for various glass formers (Refs. 15 and 16). The solid line is a guide for the eye drawn through the data for the glass formers without hydrogen bonds.

B. The boson peak

The origin of the boson peak has been much discussed recently.[1] Suggestions range from localization of phonons when the wavelength is comparable to the typical length scale for structural disorder, to cluster type modes. In the present case the boson peak is clearly seen at low temperatures but becomes completely covered by a quasielastic contribution at high temperatures (>240 K), see Fig. 6. The behavior is markedly different from strong glass formers such as B_2O_3 (Ref. 16) and GeO_2 (Ref. 38) for which the boson peak is observed well above the glass transition temperature.

C. The α' relaxation

The PCS measurements on PPG show that the relaxation function just above T_g is well described by a KWW function but at higher temperatures a long-time tail appears (see Fig. 5). We note that the dynamical features of this additional process is similar to what is found in dielectric spectroscopy for the α' relaxation, i.e., similar stretching of the time decay and roughly the same temperature dependence of the relaxation time though the experimental scatter of the PCS data make any quantative analysis vague. This additional process might be due to the so-called normal mode motions of the polymer chain.[39] The dielectric data have shown that the relaxation time of this process is M_W dependent, in accordance with Rouse dynamics, and in contrast to the M_W independent α process for PPG of $M_W>400$. However, the M_W dependence were shown to be affected by the OH end groups

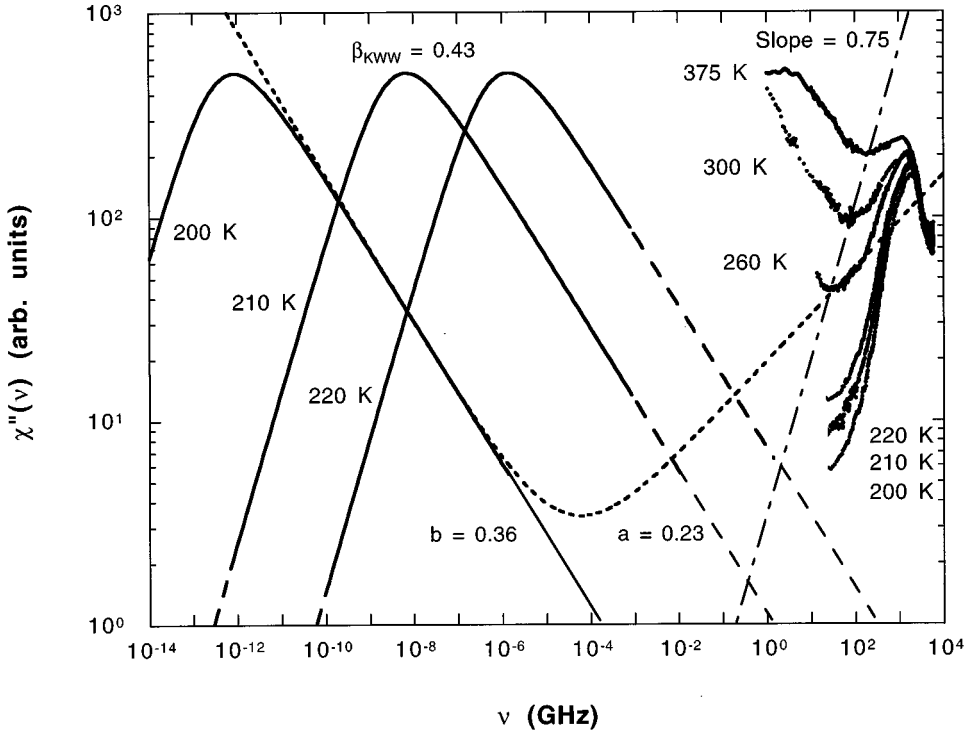

FIG. 10. Combined depolarized Raman and Brillouin data (high frequencies) together with Havriliak-Negami representations of KWW relaxation functions fitted to the time domain PCS data. The solid curves represent the approximate range covered by PCS. The dotted curve represents MCT interpolation [Eq. (7)]. The dashed curves extend the Havriliak-Negami function to higher frequencies. The dash-dotted line represents the temperature dependence of the frequency dependence of the susceptibility minima, as obtained from Fig. 8. The joining of the low- and high-frequency regions is only approximate. The β relaxations were interpolated using MCT [Eq. (7)] with the a and b values as obtained from the analysis of the PCS data, and scaled to the minimum of the high-frequency data taken at 260 K (the lowest temperature for which we can discern a minimum).

which links PPG chains via hydrogen bonds and thus producing a longer effective chain. Light-scattering measurements of PPG with different molecular weights and with the OH end groups replaced by CH_3 end groups to elucidate the M_W dependence is currently being performed.

We note that the dielectric α and α' double-peak scenario in PPG has been explained by Fuchs *et al.* within the framework of MCT (Ref. 20) and also by Ngai *et al.* using the coupling model.[40]

VI. CONCLUSIONS

The structural dynamics of PPG has been investigated over wide dynamical ranges using light-scattering techniques. A rather complex behavior is observed. The slow structural relaxation observed close to T_g in the time domain using the photon correlation technique is found to closely adhere to the MCT relaxation scenario with exponents $a = 0.23 \pm 0.05$ and $b = 0.36 \pm 0.02$, which in accordance with MCT gives a common λ value within the experimental error. Moreover, the high-temperature viscosity data can be well described using the MCT power law [Eq. (5)] with $T_c \approx 236$ K and an exponent γ calculated from the obtained λ value. This result is in accordance with the analysis of dielectric data on PPG by Fuchs *et al.*[20]

The data from the frequency domain obtained from combined Raman and Brillouin measurements show a minimum in the high-frequency susceptibility spectra which can be described by an interpolation formula as suggested in MCT. However, the high-frequency susceptibilities are too influenced by the boson vibrational peak to give results consistent with the MCT. This observation has also been made in recent experiments on hydrogen bonded or strong covalently bonded glass formers.[15,16,41,42]

Thus, we observe a relaxation scenario qualitatively in accordance with MCT, i.e., an α-relaxation peak moving towards a high-frequency peak as temperature increases. We have shown that the dynamic region around the plateau (in time domain) or the minimum (in frequency domain) can be described by the MCT interpolation formulas. However, the exponents obtained at high temperatures and frequencies do not obey the MCT predictions. Moreover, the intensity at the high-frequency side of the minimum decreases strongly with temperature also below T_c contrary to MCT. Finally, at times longer than that of the α relaxation we observe a slower process which we attribute to normal modes relaxation of the whole chain, the so-called α' relaxation.

We conclude that MCT at present cannot fully describe the dynamics of the polymer, poly(propylene glycol), deviations being observed in the short-time dynamics close to the Boson peak.

ACKNOWLEDGMENTS

We are indebted to Dr. A. Schönhals for kindly providing his results from dielectric measurements on PPG. This work was supported by the Swedish Natural Science Research Council.

[1] *Proceedings of the Second International Discussion Meeting on Relaxations in Complex Systems*, edited by K. L. Ngai, E. Riande, and G. B. Wright, J. Non-Cryst. Solids **172–174** (1994).
[2] C. A. Angell, J. Non-Cryst. Solids **131–133**, 13 (1991).
[3] R. Böhmer, K. L. Ngai, C. A. Angell, and D. J. Plazek, J. Chem. Phys. **99**, 4201 (1993).
[4] W. Götze and L. Sjögren, Rep. Prog. Phys. **55**, 241 (1992).
[5] U. Bengtzelius, W. Götze, and A. Sjölander, J. Phys. C **17**, 5915 (1984).
[6] U. Bengtzelius, W. Götze, and A. Sjölander, Phys. Rev. A **34**, 5059 (1986).
[7] E. Leutheusser, Phys. Rev. A **29**, 2765 (1984).
[8] S. Yip, *Special Issue Devoted to Relaxation Kinetics in Supercooled Liquids-Mode Coupling Theory and Its Experimental Tests, Transport Theory and Statistical Physics* (Marcel Dekker, Inc., New York, 1995), Vol. 24.
[9] E. Bartsch, Transp. Theory Stat. Phys. **24**, 1125 (1995).
[10] W. van Megen, Transp. Theory Stat. Phys. **24**, 1017 (1995).
[11] C. A. Angell, in *Relaxations in Complex Systems*, edited by K. L. Ngai and G. B. Wright (National Technical Information Service, U.S. Department of Commerce, Springfield, VA, 1985), p. 3.
[12] C. A. Angell, Nucl. Phys. B **5**, 69 (1988).
[13] C. A. Angell, J. Phys. Chem. Solids **49**, 863 (1988).
[14] J. Wuttke, J. Hernandez, G. Li, G. Coddens, H. Z. Cummins, F. Fujara, W. Petry, and H. Sillescu, Phys. Rev. Lett. **72**, 3052 (1994).
[15] A. P. Sokolov, W. Steffen, and E. Rössler, Phys. Rev. E **52**, 5105 (1995).
[16] A. Brodin, L. Börjesson, D. Engberg, L. M. Torell, and A. P. Sokolov, Phys. Rev. B **53**, 11 511 (1996).
[17] K. S. Schweizer and G. Szamel, Philos. Mag. B **71**, 783 (1995).
[18] K. S. Schweizer, J. Chem. Phys. **91**, 5822 (1989).
[19] F. Mezei, W. Knaak, and B. Farago, Phys. Rev. Lett. **58**, 571 (1987).
[20] M. Fuchs, W. Götze, I. Hofacker, and A. Latz, J. Phys. Condens. Matter **3**, 5047 (1991).
[21] D. L. Sidebottom, R. Bergman, L. Börjesson, and L. M. Torell, Phys. Rev. Lett. **68**, 3587 (1992).
[22] C. H. Wang, G. Fytas, D. Lilge, and T. Dorfmüller, Macromolecules **14**, 1363 (1981).
[23] B. Kim and G. F. Mazenko, Phys. Rev. B **45**, 2393 (1992).
[24] P. K. Dixon, L. Wu, S. R. Nagel, B. D. Williams, and J. P. Carini, Phys. Rev. Lett. **65**, 1108 (1990).
[25] L. M. Torell, L. Börjesson, and M. Elmroth, J. Phys. Condens. Matter **2**, SA207 (1990).
[26] A. Schönhals, F. Kremer, and E. Schlosser, Phys. Rev. Lett. **67**, 999 (1991).
[27] J. Yeo and G. F. Mazenko, Phys. Rev. E **51**, 5752 (1995).
[28] R. Schmitz, J. W. Dufty, and P. De, Phys. Rev. Lett. **71**, 2066 (1993).
[29] G. Fytas and G. Meier, in *Dynamic Light Scattering*, edited by W. Brown (Clarendon Press, Oxford, 1993), pp. 407–439.
[30] A. Schönhals and E. Schlosser, Phys. Scr. **T49**, 233 (1993).
[31] A. Schönhals (private communication).
[32] L. Börjesson, J. R. Stevens, and L. M. Torell, Polymer **28**, 1803 (1987).
[33] A. R. Duggal and K. A. Nelson, J. Chem. Phys. **94**, 7677 (1991).
[34] G. P. Johari, Polymer **27**, 866 (1986).
[35] W. Götze and L. Sjögren, Transp. Theory Stat. Phys. **24**, 801 (1995).
[36] F. Alvarez, A. Alegria, and J. Colmenero, Phys. Rev. B **44**, 7306 (1991).
[37] F. Alvarez, A. Alegria, and J. Colmenero, Phys. Rev. B **47**, 125 (1993).
[38] A. Brodin and L. M. Torell, J. Raman Spectrosc. **27**, 723 (1996).
[39] M. E. Baur and W. H. Stockmayer, J. Chem. Phys. **43**, 4319 (1965).
[40] K. L. Ngai, A. Schönhals, and E. Schlosser, Macromolecules **25**, 4915 (1992).
[41] J. Wuttke, J. Hernandez, G. C. G. Li, H. Z. Cumminz, F. Fujara, W. Petry, and H. Sillescu, Phys. Rev. Lett. **72**, 3052 (1994).
[42] M. J. Lebon, C. Dreyfus, G. Li, A. Aouadi, H. Z. Cumminz, and R. M. Pick, Phys. Rev. B **51**, 4537 (1995).